Ordered Spin Ice State and Magnetic Fluctuations in $Tb_2Sn_2O_7$

I. Mirebeau,[1] A. Apetrei,[1] J. Rodríguez-Carvajal,[1] P. Bonville,[2] A. Forget,[2] D. Colson,[2] V. Glazkov,[3] J. P. Sanchez,[3] O. Isnard,[4,5] and E. Suard[5]

[1]*Laboratoire Léon Brillouin, CEA-CNRS, CE-Saclay, 91191 Gif-sur-Yvette, France*
[2]*Service de Physique de l'Etat Condensé, CEA-CNRS, CE-Saclay, 91191 Gif-Sur-Yvette, France*
[3]*Service de Physique Statistique, Magnétisme et Supraconductivité, CEA-Grenoble, 38054 Grenoble, France*
[4]*Laboratoire de Cristallographie, Université J. Fourier–CNRS, BP 166, 38042 Grenoble, France*
[5]*Institut Laüe Langevin, 6 rue Jules Horowitz, BP 156X, 38042 Grenoble, France*

(Received 17 January 2005; published 21 June 2005)

We have studied the spin liquid $Tb_2Sn_2O_7$ by neutron diffraction and specific heat measurements. Below about 2 K, the antiferromagnetic liquidlike correlations mostly change to ferromagnetic. Magnetic order settles in two steps, with a smeared transition at 1.3(1) K, then an abrupt transition at 0.87(2) K. A new magnetic structure is observed, akin to an ordered spin ice, with both ferromagnetic and antiferromagnetic character. It suggests that the ordered ground state results from the influence of dipolar interactions combined with a finite anisotropy along $\langle 111 \rangle$ axes. The moment value of $3.3(3)\mu_B$ deduced from the specific heat is well below that derived from the neutron diffraction of $5.9(1)\mu_B$, which is interpreted by the persistence of slow collective magnetic fluctuations down to the lowest temperatures.

DOI: 10.1103/PhysRevLett.94.246402 PACS numbers: 71.27.+a, 61.12.Ld, 75.25.+z

Geometrically frustrated pyrochlores $R_2Ti_2O_7$ show exotic magnetic behaviors [1–4] such as dipolar spin ice (R = Dy, Ho) and spin liquid (Tb) phases, a first order transition in the spin dynamics (Yb), or complex antiferromagnetic (AFM) orders (Er, Gd). The type of magnetic order depends on the balance between antiferromagnetic exchange, dipolar, and crystal field energies [5,6]. $Tb_2Ti_2O_7$ is a unique case of a spin liquid where short-ranged correlated magnetic moments fluctuate down to 70 mK, with typical energies 300 times lower than the energy scale given by the Curie-Weiss constant θ_{CW} of -19 K. The fact that $Tb_2Ti_2O_7$ does not order at ambient pressure [2], but can order under applied pressure, stress, and magnetic field [7,8], is still a challenge to theory, since recent models predict a transition towards antiferromagnetic long range order at about 1 K [9,10].

With respect to titanium, substitution by tin yields a lattice expansion. It also modifies the oxygen environment of the Tb^{3+} ion and therefore the crystal field. The stannates $R_2Sn_2O_7$ show the same crystal structure [11] as the titanates, and susceptibility data [12,13] also suggest a great variety of magnetic behaviors. $Dy_2Sn_2O_7$ and $Ho_2Sn_2O_7$ are dipolar spin ices [14,15] like their Ti parent compounds, whereas $Er_2Sn_2O_7$ does not order down to 0.15 K [13], and $Gd_2Sn_2O_7$ undergoes a transition to AFM order [16]. In $Tb_2Sn_2O_7$, magnetic measurements suggest an original and complex behavior. Antiferromagnetic interactions are observed at high temperature, yielding a Curie-Weiss constant θ_{CW} of -11 to -12 K [12,13], but a ferromagnetic (FM) transition is seen around 0.87 K [13].

We have performed neutron diffraction and specific heat measurements in $Tb_2Sn_2O_7$. With decreasing temperature, a spin liquid phase is shown to transform into a new type of ordered phase, not predicted by theory, which could be called an ''ordered spin ice.'' Just above the transition, an abnormal change in the spin correlations shows the influence of dipolar interactions. By comparing the ordered Tb^{3+} moment values from neutron diffraction and nuclear specific heat, we also indirectly observe slow fluctuations of correlated spins, which persist down to the lowest temperature.

The crystal structure of $Tb_2Sn_2O_7$ with space group $Fd\bar{3}m$ was studied at 300 K by combining powder x-ray and neutron diffraction, the neutron pattern being measured in the diffractometer 3T2 of the Laboratoire Léon Brillouin (LLB). Rietveld refinements performed with FULLPROF [17] confirmed the structural model (R_B = 2.4%), yielding the lattice constant $a = 10.426$ Å and oxygen position parameter $x = 0.336$. The magnetic diffraction patterns were recorded between 1.4 and 300 K and down to 0.1 K in the diffractometer G6-1 (LLB) and D1B of the Institut Laüe Langevin (ILL), respectively. The specific heat was measured by the dynamic adiabatic method down to 0.15 K.

Figure 1 shows magnetic neutron diffraction patterns for several temperatures. The liquidlike peak corresponding to AFM first neighbor correlations [18] starts to grow below 100 K. Below 2 K, it narrows and slightly shifts, and an intense magnetic signal appears at low q values. This shows the onset of ferromagnetic correlations, which progressively develop as the temperature decreases. Below 1.2 K, a magnetic contribution starts to appear on the Bragg peaks of the face centered cubic (fcc) lattice, which steeply increases at 0.87(2) K. This shows the onset of an ordered magnetic phase with a propagation vector $\mathbf{k} = 0$.

Rietveld refinements of the magnetic diffraction patterns (Fig. 2) were performed with FULLPROF [17]. The magnetic

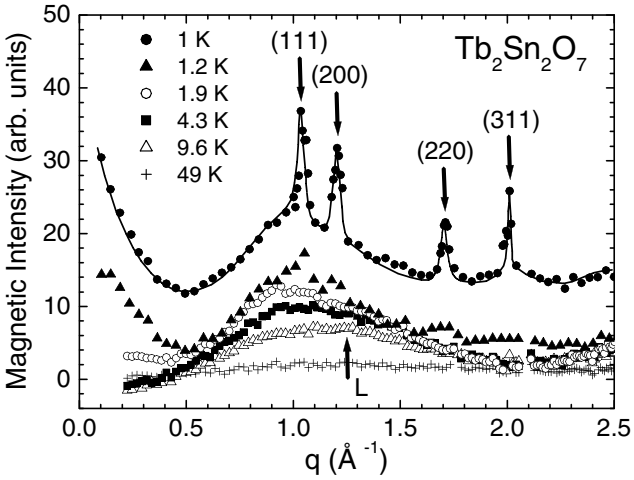

FIG. 1. Magnetic intensity of $Tb_2Sn_2O_7$ versus the scattering vector $q = 4\pi \sin\theta/\lambda$. A spectrum in the paramagnetic phase (100 K) was subtracted. Intensities at 1.0 K have an offset of 10 for clarity. Arrows show the position of the Bragg peaks and near neighbor liquid peak (L) calculated in Ref. [18].

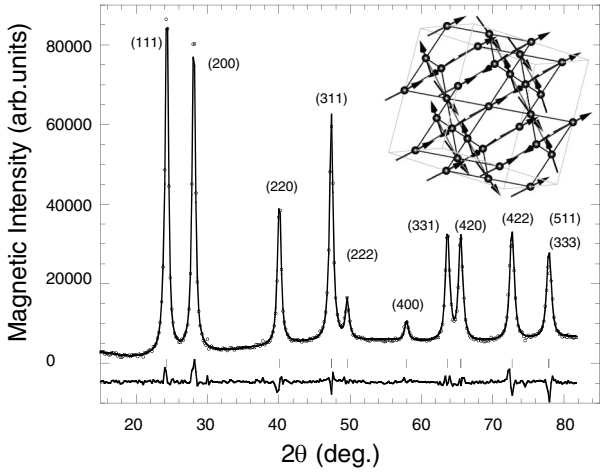

FIG. 2. Magnetic diffraction pattern of $Tb_2Sn_2O_7$ at 0.10 K versus the scattering angle 2θ. A spectrum at 1.2 K was subtracted. The neutron wavelength is 2.52 Å. Solid lines show the best refinement and the difference spectrum (bottom). In the inset, the magnetic structure is shown.

structure was solved by a systematic search, using the program BASIREPS [19] and symmetry-representation analysis [20]. The basis states describing the Tb^{3+} magnetic moments were identified and the symmetry allowed structures were compared to experiment. Neither a collinear ferromagnetic structure nor the $\mathbf{k} = 0$ AFM structures allowed by $Fd\bar{3}m$ symmetry were compatible with the data, yielding extinctions of several Bragg peaks. This suggests a magnetic component breaking the $Fd\bar{3}m$ symmetry. Then we searched for all solutions in the space group $I4_1/amd$, the highest subgroup allowing FM and AFM components simultaneously. The best refinement [21] ($R_B = 2.3\%$) is shown in Fig. 2 and Table I.

In the ordered structure with $\mathbf{k} = 0$, the four tetrahedra of the cubic unit cell are equivalent. In a given tetrahedron, the Tb^{3+} moments make an angle $\alpha = 13.3°$ with the local $\langle 111 \rangle$ anisotropy axes connecting the center to the vertices. The components along these $\langle 111 \rangle$ axes are oriented in the "two in, two out" configuration of the local spin-ice structure [1]. The ferromagnetic component, which represents 37% of the Tb^{3+} ordered moment, orders in magnetic domains oriented along $\langle 100 \rangle$ axes. The perpendicular components make two couples of antiparallel vectors along $\langle 110 \rangle$ edge axes of the tetrahedron. The ordered moment [$M = 5.9(1)\mu_B$ at 0.1 K] is reduced with respect to the free ion moment of $9\mu_B$ as expected from crystal field effects. With increasing temperature, M remains almost constant up to 0.6 K. Then it steeply decreases, showing an inflection point which coincides with the T_c value of 0.87(2) K determined from the peaks in the specific heat and susceptibility [13], and finally vanishes at 1.3(1) K (Fig. 3). The magnetic correlation length L_c was deduced from the intrinsic peak linewidth [17]. L_c remains constant and limited to about 190 Å up to T_c, and then starts to decrease above T_c. The angle α is constant within the experimental error.

The magnetic ground state results from a delicate balance between exchange, dipolar, and anisotropy energies. Several theories were developed involving the AFM nearest neighbor exchange J_{nn}, the FM nearest neighbor dipolar coupling D_{nn}, and the strength of the local anisotropy D_a (all taken in absolute values). A spin liquid ground state is predicted for AFM exchange only and Heisenberg spins [22], namely, for $J_{nn} \gg D_{nn}, D_a$. The dipolar spin-ice state is stabilized for Ising spins when dipolar interactions overcome the AFM exchange [23,24], namely, for $D_a \gg D_{nn} > J_{nn}$. Its local spin structure is similar to the present one, but spins keep the orientational disorder allowed by the "ice rules." When either a finite anisotropy [25] ($J_{nn} \geq D_a \gg D_{nn}$) or a small dipolar coupling [6] ($D_a \gg J_{nn} > D_{nn}$) is considered, a $\mathbf{k} = 0$ structure is predicted, but with a different local order, where all spins of a tetrahedron point either "in" or "out." For Heisenberg spins when dipolar interactions dominate ($D_{nn} > J_{nn} \gg D_a$) a $\mathbf{k} = 0$ structure is predicted, but the local spin structure consists of antiparallel moments along the $\langle 110 \rangle$ edge axes of the

TABLE I. Magnetic components M_x, M_y, and M_z of the four Tb^{3+} moments (in μ_B) in one tetrahedron at 0.1 K. The atomic coordinates x, y, z and the magnetic components are expressed in the cubic unit cell.

Site	x	y	z	M_x	M_y	M_z
1	0.5	0.5	0.5	3.85 (1)	3.85 (1)	2.20 (1)
2	0.25	0.25	0.5	−3.85 (1)	−3.85 (1)	2.20 (1)
3	0.25	0.5	0.25	3.85 (1)	−3.85 (1)	2.20 (1)
4	0.5	0.25	0.25	−3.85 (1)	3.85 (1)	2.20 (1)

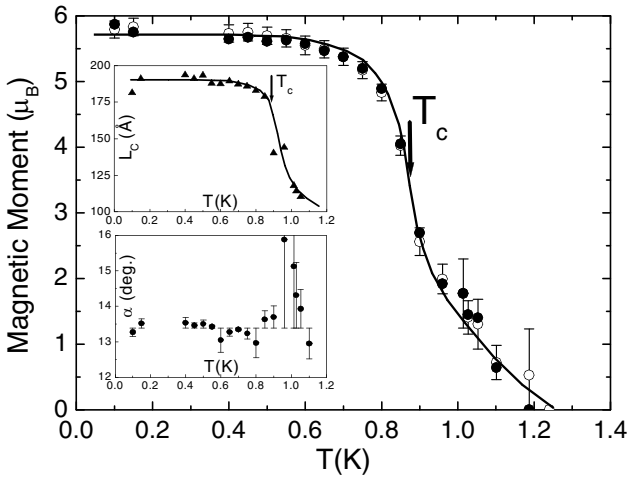

FIG. 3. Ordered magnetic moment M versus temperature (filled circles) and squared intensity of the (200) magnetic peak, scaled to the moment at 0.10 K (open circles). T_c is determined from the peak in the specific heat. The correlation length L_c, deduced from the width of the magnetic Bragg peaks, and the angle α with the local anisotropy axis are plotted in the insets.

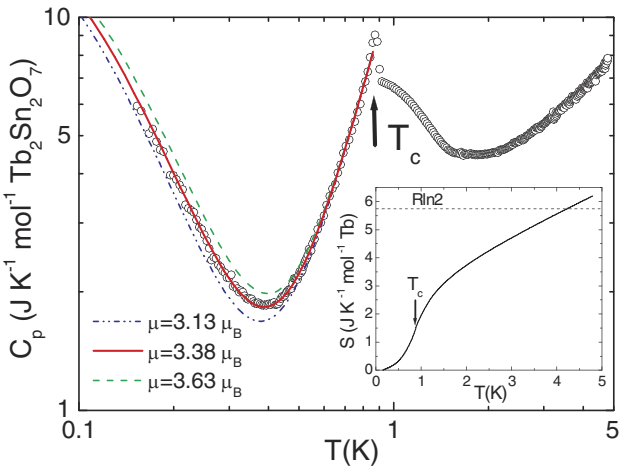

FIG. 4 (color online). Specific heat C_p in $Tb_2Sn_2O_7$. The curves below 0.8 K are the sum of a T^3 magnon contribution and of a nuclear Schottky anomaly, the latter being computed for 3 moment values (see text). The electronic entropy variation is shown in the inset. The arrows label the transition at $T_c = 0.87$ K.

tetrahedron [26]. For an easy plane anisotropy ($D_a < 0$), the local order selected for the $\mathbf{k} = 0$ structure, which is actually observed in $Er_2Ti_2O_7$, is also different [4]. The ordered state of $Tb_2Sn_2O_7$ rather resembles that predicted for a *ferromagnetic* first neighbor exchange interaction combined with a finite anisotropy along $\langle 111 \rangle$ axes [27]. It suggests that in $Tb_2Sn_2O_7$ the magnetic order results from an effective ferromagnetic interaction resulting from AFM exchange and FM dipolar coupling, the strength of the uniaxial anisotropy tuning the angle α. This may happen if $D_{nn} > D_a > J_{nn}$. The unusual change with temperature in the short range correlations from AFM to FM, which occurs just above the transition, also suggests that it is driven by an effective ferromagnetic interaction, which should naturally result from the influence of dipolar coupling [28] as in dipolar spin ices.

The temperature dependence of the specific heat C_p is shown in Fig. 4. In good agreement with neutron diffraction data, the specific heat C_p starts to increase below about 1.5 K, and then shows a well defined peak at 0.87 K. The final increase of C_p below 0.38 K is attributed to a nuclear Schottky anomaly, resulting from the splitting of the energy levels of the ^{159}Tb nuclear spin ($I = 3/2$) by the hyperfine field due to the Tb^{3+} electronic moment. The whole nuclear Schottky peak was observed in Tb_2GaSbO_7 [29]. The nuclear Schottky anomaly C_{nuc} was calculated as follows: the full hyperfine Hamiltonian, i.e., the Zeeman part due to the hyperfine field H_{hf} and a quadrupolar term, was diagonalized to obtain the four hyperfine energies. The small quadrupolar term is the sum of a lattice contribution, extrapolated from that measured in $Gd_2Sn_2O_7$ [30] and of an estimated $4f$ term, both amounting to about 5% of the magnetic term. The angle the hyperfine field is at the local $\langle 111 \rangle$ axis was fixed at the value 13.3°. The H_{hf} value then is the only parameter for the calculation of C_{nuc}, which was obtained using the standard expression for a Schottky anomaly. The lines in Fig. 4 below 0.8 K represent $C_p = C_{nuc} + C_m$, where $C_m = \beta\, T^3$ is an empirical electronic magnon term which fits well the rise of C_p above 0.4 K, with $\beta = 12.5\ \mathrm{J\,K^{-4}\,mol^{-1}}$. The best fit to the data is obtained with a hyperfine field of 135 T, which corresponds to a Tb^{3+} moment value of $3.3(3)\mu_B$, using the hyperfine constant of 40(4) T/μ_B. The electronic entropy variation S was computed by integrating $(C_p - C_{nuc})/T$ (inset of Fig. 4). In $Tb_2Sn_2O_7$, our current measurements show that the crystal field level scheme is only slightly modified with respect to that in $Tb_2Ti_2O_7$, where the lowest states are two doublets separated by 18 K [31]. Therefore S should reach the values $R\ln 2$ and $R\ln 4$ when T increases above T_c, as the first two doublets become populated. In fact, the entropy released at the transition is only 25% of $R\ln 2$, and it reaches 50% of $R\ln 2$ at 1.5 K. This reflects the strong correlations of the magnetic moments in the spin liquid phase above 1.5 K.

The value $m_{eff} = 3.3(3)\mu_B$ for the Tb moment deduced from the nuclear specific heat is therefore well below the neutron value $M = 5.9(1)\mu_B$. Such a remarkable reduction can be explained by the presence of electronic fluctuations, if their characteristic time τ is comparable to the spin-lattice nuclear relaxation time T_1 which governs the thermalization of the hyperfine levels, as in $Gd_2Sn_2O_7$ [30]. Within this model [30], the reduction factor of the nuclear Schottky anomaly is $1 + 2T_1/\tau$, to be compared with the experimental reduction proportional to $(m_{eff}/M)^2 \simeq 0.3$. Then a ratio $T_1/\tau \simeq 1$ can be inferred in $Tb_2Sn_2O_7$. This

implies low temperature fluctuations of the Tb^{3+} moments with a time scale 10^{-4}–10^{-5} s, much slower than for paramagnetic spins (10^{-11} s), which means that these fluctuations involve correlated spins, as previously noticed in geometrically frustrated magnets [23]. Here, they occur in magnetically ordered domains and may be connected with their finite size. They could be probed by muon spin relaxation experiments.

Why does $Tb_2Sn_2O_7$ order and not $Tb_2Ti_2O_7$? The weaker AFM exchange of $Tb_2Sn_2O_7$ may not be the only reason. Our current crystal field study of the two compounds by high resolution neutron scattering points out another fact. In $Tb_2Sn_2O_7$ only, we have observed a small splitting (1.5 K) of a low energy excitation. It shows a lifting of the degeneracy of a crystal field doublet, possibly due to the higher value of the oxygen parameter which controls the local distortion around the Tb^{3+} ion. Assuming that the spectral density of the spin fluctuations decreases with energy, this lifting could weaken in $Tb_2Sn_2O_7$ the quantum fluctuations responsible for the persistence of the spin liquid state in $Tb_2Ti_2O_7$, and allow long range order to set in.

In conclusion, we observed a new magnetic structure in the spin liquid $Tb_2Sn_2O_7$. This unpredicted structure with both ferromagnetic and antiferromagnetic character could be called an ''ordered dipolar spin ice.'' It arises below 1.3(1) K with a low ordered moment and strong fluctuations. Then at 0.87 K a steep increase of the ordered moment coincides with a peak in the specific heat. In the spin liquid phase, ferromagnetic correlations start to replace antiferromagnetic ones below about 2 K. In the ground state, the lower Tb^{3+} moment estimated from specific heat shows that the hyperfine levels are out of equilibrium and evidences the persistence of slow magnetic fluctuations of correlated spins. These unconventional fluctuations are reminiscent of the spin liquid in the ordered phase.

We thank F. Bourée for the neutron measurement on the diffractometer 3T2, as well as R. Moessner and M. J. P. Gingras for interesting comments. We also thank F. Thomas and the cryogenic team of the ILL.

[1] M. J. Harris *et al.*, Phys. Rev. Lett. **79**, 2554 (1997).
[2] J. S. Gardner *et al.*, Phys. Rev. Lett. **82**, 1012 (1999).
[3] J. A. Hodges *et al.*, Phys. Rev. Lett. **88**, 077204 (2002).
[4] J. D. M. Champion *et al.*, Phys. Rev. B **64**, 140407(R) (2001); **68**, 020401(R) (2003).
[5] R. Siddharthan *et al.*, Phys. Rev. Lett. **83**, 1854 (1999).
[6] B. C. den Hertog and M. J. P. Gingras, Phys. Rev. Lett. **84**, 3430 (2000).
[7] I. Mirebeau, I. N. Goncharenko, P. Cadavez-Peres, S. T. Bramwell, M. J. P. Gingras, and J. S. Gardner, Nature (London) **420**, 54 (2002).
[8] I. Mirebeau, I. N. Goncharenko, G. Dhalenne, and A. Revcolevschi, Phys. Rev. Lett. **93**, 187204 (2004).
[9] Y. J. Kao *et al.*, Phys. Rev. B **68**, 172407 (2003).
[10] M. Enjalran *et al.*, J. Phys. Condens. Matter **16**, S673 (2004).
[11] B. J. Kennedy, B. A. Hunter, and C. J. Howard, J. Solid State Chem. **130**, 58 (1997).
[12] V. Bondah-Jagalu and S. T. Bramwell, Can. J. Phys. **79**, 1381 (2001).
[13] K. Matsuhira *et al.*, J. Phys. Soc. Jpn. **71**, 1576 (2002).
[14] K. Matsuhira, H. Hinatsu, K. Tenya, and T. Sakakibara, J. Phys. Condens. Matter **12**, L649 (2000).
[15] H. Kadowaki, Y. Ishii, K. Matsuhira, and Y. Hinatsu, Phys. Rev. B **65**, 144421 (2002).
[16] P. Bonville *et al.*, J. Phys. Condens. Matter **15**, 7777 (2003).
[17] J. Rodríguez-Carvajal, Physica (Amsterdam) **192B**, 55 (1993).
[18] B. Canals and D. A. Garanin, Can. J. Phys. **79**, 1323 (2001).
[19] J. Rodríguez-Carvajal, BASIREPS, ftp://ftp.cea.fr/pub/llb/divers/BasIreps.
[20] Y. A. Izyumov, V. E. Naish, and R. P. Ozerov, *Neutron Diffraction on Magnetic Materials* (Consultants Bureau, New York, 1991).
[21] The magnetic structure is obtained for a state described as a linear combination of the two basis vectors of the irreducible representation Γ_7. To obtain the list of irreducible representations and basis functions for the case $I4_1/amd$ and $\mathbf{k} = 0$, one has to run the program BASIREPS using the coordinates of Tb atoms (0, 0.5, 0.5), (0, 0, 0.5), (−0.25, 0.25, 0.25), (0.25, 0.25, 0.25).
[22] J. N. Reimers, A. J. Berlinsky, and A. C. Shi, Phys. Rev. B **43**, 865 (1991).
[23] S. T. Bramwell *et al.*, Phys. Rev. Lett. **87**, 047205 (2001).
[24] S. T. Bramwell and M. J. P. Gingras, Science **294**, 1495 (2001).
[25] R. Moessner, Phys. Rev. B **57**, R5587 (1998).
[26] S. E. Palmer and J. T. Chalker, Phys. Rev. B **62**, 488 (2000).
[27] J. D. M. Champion, S. T. Bramwell, P. C. W. Holdsworth, and M. J. Harris, Europhys. Lett. **57**, 93 (2002).
[28] R. G. Melko and M. J. P. Gingras, J. Phys. Condens. Matter **16**, R1277 (2004).
[29] H. W. J. Blöte, R. F. Wielinga, and W. J. Huiskamp, Physica (Amsterdam) **43**, 549 (1969).
[30] E. Bertin, P. Bonville, J. P. Bouchaud, J. A. Hodges, J. P. Sanchez, and P. Vuillet, Eur. Phys. J. B **27**, 347 (2002).
[31] M. J. P. Gingras *et al.*, Phys. Rev. B **62**, 6496 (2000).